

## Ferrimagnetic Fe<sup>III</sup>–Mn<sup>III</sup> Zigzag Chain Formed by a New *mer*-Positioned Iron(III) Cyanide Precursor

Jae Il Kim,<sup>†</sup> Houn Sik Yoo,<sup>†</sup> Eui Kwan Koh,<sup>‡</sup> Hyoung Chan Kim,<sup>§</sup> and Chang Seop Hong<sup>\*†</sup>

Department of Chemistry, Korea University, Seoul 136-713, Korea, Nano-Bio System Research Team, Korea Basic Science Institute, Seoul 136-713, Korea, and Research & Development Division, Nuclear Fusion Research Center, Daejeon 305-333, Korea

Received July 9, 2007

A new cyanide-bearing molecular precursor, *mer*-[Fe(pzcq)(CN)<sub>3</sub>]<sup>−</sup> (**1**), and a zigzag chain, [Fe(pzcq)(CN)<sub>3</sub>][Mn(salen)]·4H<sub>2</sub>O (**2**), were prepared and characterized in terms of structure and magnetism. Magnetic data reveal that intrachain antiferromagnetic couplings via cyanide ligands in **2** are clearly operating, resulting in a ferrimagnetic nature.

Extensive works on low-dimensional magnetic materials have been carried out because of the fundamental interest (quantum tunneling of magnetization, for example) and their potential applications in magnetic information storage materials. To attain these systems, the employment of capped molecular entities [ML<sub>p</sub>(CN)<sub>q</sub>]<sup>n−</sup> (M = paramagnetic metal ions; L = polydentate ligand) is appropriate because the precursors with chelating ligands can control the structural evolution in constrained directions and, as a result, generate low-dimensional magnetic assemblies.<sup>1</sup> Among them, the Fe<sup>III</sup> complexes have attracted special attention because they serve as magnetic anisotropic sources. Some of the pertinent building blocks used to date are [Fe(A)(CN)<sub>4</sub>]<sup>−</sup> [A = bidentate nitrogen donor; 2,2′-bipyridine (bpy); 1,10-phenanthroline (phen); 2,2′-bipyrimidine (bpym)],<sup>2–4</sup> *fac*-[Fe(B)(CN)<sub>3</sub>]<sup>−</sup> (B = facially coordinate tridentate ligand; hydrotris(pyrazolyl)borate (Tp); hydrotris(3,5-dimethylpyrazol-1-yl)borate (Tp\*); tetra(pyrazol-1-yl)borate (pzTp); tach =

1,3,5-triaminocyclohexane (tach)),<sup>5–9</sup> *mer*-[Fe(C)(CN)<sub>3</sub>]<sup>−</sup> [C = meridionally coordinate tridentate ligand; bis(2-pyridyl-carbonyl)amidate anion (bpca); 8-(pyridine-2-carboxamido)quinoline anion (pcq)],<sup>10,11</sup> and [Fe(D)(CN)<sub>2</sub>]<sup>−</sup> [D = tetradentate ligand; 1,2-bis(pyridine-2-carboxamido)benzenate (bpb)].<sup>12</sup> On the other hand, Mn<sup>III</sup> Schiff bases with enhanced Jahn–Teller effects are also other anisotropic origins to fabricate such complexes. Thus, the combination of both anisotropic molecular precursors would be one of the rational strategies to achieve intriguing low-dimensional entities.

Herein we report the synthesis, structures, and magnetic properties of a new molecular building unit, (PPh<sub>4</sub>)[Fe(pzcq)(CN)<sub>3</sub>] [**1**; pzcq = 8-(pyrazine-2-carboxamido)quinoline anion], and a one-dimensional bimetallic chain, [Fe(pzcq)(CN)<sub>3</sub>][Mn(salen)]·4H<sub>2</sub>O [**2**; salen = *N,N*-ethylenebis(salicylideneiminato) dianion]. It is worth noting that **2** is the first example of the cyanide-bridged Fe<sup>III</sup>–Mn<sup>III</sup> ferrimagnetic chain constructed by the low-spin Fe<sup>III</sup> precursor bearing three CN ligands with a *mer* arrangement and the Mn<sup>III</sup> Schiff base.<sup>2–4,9</sup>

A stoichiometric reaction of [Fe(pzcq)(CN)<sub>3</sub>]<sup>−</sup> and [Mn(salen)(H<sub>2</sub>O)](ClO<sub>4</sub>) in MeOH gave brown crystals of **2** in good yield.<sup>13</sup> No Cl–O stretching vibrations in the IR

\* To whom correspondence should be addressed. E-mail: cshong@korea.ac.kr.

<sup>†</sup> Korea University.

<sup>‡</sup> Korea Basic Science Institute.

<sup>§</sup> Nuclear Fusion Research Center.

- (1) (a) Lescouëzec, R.; Toma, L. M.; Vaissermann, J.; Verdager, M.; Delgado, F. S.; Ruiz-Pérez, C.; Lloret, F.; Julve, M. *Coord. Chem. Rev.* **2005**, *249*, 2691. (b) Sokol, J. J.; Hee, A. G.; Long, J. R. *J. Am. Chem. Soc.* **2002**, *124*, 7656. (c) Yoon, J. H.; Lim, J. H.; Choi, S. W.; Kim, H. C.; Hong, C. S. *Inorg. Chem.* **2007**, *46*, 1529.
- (2) Toma, L. M.; Lescouëzec, R.; Lloret, F.; Julve, M.; Vaissermann, J.; Verdager, M. *Chem. Commun.* **2003**, 1850.
- (3) Lescouëzec, R.; Vaissermann, J.; Ruiz-Pérez, C.; Lloret, F.; Carrasco, R.; Julve, M.; Verdager, M.; Dromzee, Y.; Gatteschi, D.; Wernsdorfer, W. *Angew. Chem., Int. Ed.* **2003**, *42*, 1483.
- (4) Toma, L. M.; Lescouëzec, R.; Pasán, J.; Ruiz-Pérez, C.; Vaissermann, J.; Cano, J.; Carrasco, R.; Wernsdorfer, W.; Lloret, F.; Julve, M. *J. Am. Chem. Soc.* **2006**, *128*, 4842.

- (5) (a) Liu, W.; Wang, C.-F.; Li, Y.-Z.; Zuo, J.-L.; You, X.-Z. *Inorg. Chem.* **2006**, *45*, 10058. (b) Wen, H.-R.; Wang, C.-F.; Song, Y.; Gao, S.; Zuo, J.-L.; You, X.-Z. *Inorg. Chem.* **2006**, *45*, 8942. (c) Gu, Z.-G.; Yang, Q.-F.; Liu, W.; Song, Y.; Li, T.-Z.; Zuo, J.-L.; You, X.-Z. *Inorg. Chem.* **2006**, *45*, 8895. (d) Wang, S.; Zuo, J.-L.; Zhou, H.-C.; Choi, H. J.; Ke, Y.; Long, J. R.; You, X.-Z. *Angew. Chem., Int. Ed.* **2004**, *43*, 5940.
- (6) Li, D.; Parkin, S.; Wang, G.; Yee, G. T.; Prosvirnin, A. V.; Holmes, S. M. *Inorg. Chem.* **2005**, *44*, 4903.
- (7) Li, D.; Parkin, S.; Wang, G.; Yee, G. T.; Clérac, R.; Wernsdorfer, W.; Holmes, S. M. *J. Am. Chem. Soc.* **2006**, *128*, 4214.
- (8) Yang, J. Y.; Shores, M. P.; Sokol, J. J.; Long, J. R. *Inorg. Chem.* **2003**, *42*, 1403.
- (9) Wang, S.; Zuo, J.-L.; Gao, S.; Song, Y.; Zhuo, H.-C.; Zhang, Y.-Z.; You, X.-Z. *J. Am. Chem. Soc.* **2004**, *126*, 8900.
- (10) Lescouëzec, R.; Vaissermann, J.; Toma, L. M.; Carrasco, R.; Lloret, F.; Julve, M. *Inorg. Chem.* **2004**, *43*, 2234.
- (11) Ni, Z.-H.; Kou, H.-Z.; Zhang, L.-F.; Ni, W.-W.; Jiang, Y.-B.; Cui, A.-L.; Ribas, J.; Sato, O. *Inorg. Chem.* **2005**, *44*, 9631.
- (12) Ni, Z.-H.; Kou, H.-Z.; Zhao, Y.-H.; Zheng, L.; Wang, R.-J.; Cui, A.-L.; Sato, O. *Inorg. Chem.* **2005**, *44*, 2050.
- (13) See the Supporting Information.

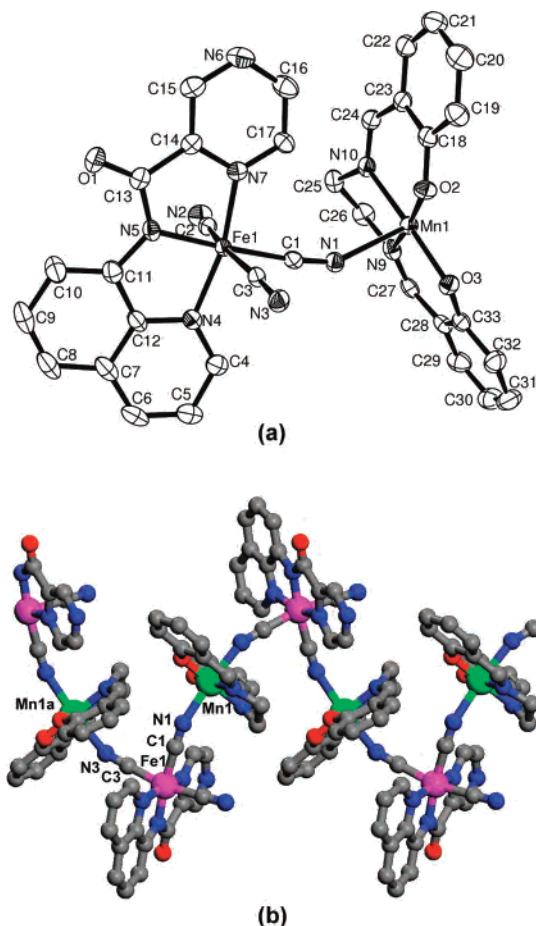


**Figure 1.** Molecular view of **2** showing (a) the atom-labeling scheme and (b) bimetallic chain structure. Symmetry code: a,  $-x + 0.5, y - 0.5, -z + 0.5$ .

spectrum indicate that the reaction is completed. The characteristic CN peaks of the molecular precursors are observed at  $2114\text{ cm}^{-1}$  (**1**) and  $2123\text{ cm}^{-1}$  for  $\text{K}[\text{Fe}(\text{pzcq})(\text{CN})_3]$ . Compound **2** has CN peaks evident at  $2143\text{ w}$  and  $2123\text{ m cm}^{-1}$ . In **2**, the first band is assignable to bridging CN groups, which is due to the peak shift toward higher frequencies compared with the precursor, and the second is due to the remaining free CN ligands.<sup>14</sup>

Both complexes crystallize in the monoclinic system as analyzed by X-ray crystallography (Figures S1 in the Supporting Information and 1).<sup>15</sup> Each Fe center of the compounds adopts a distorted octahedral environment consisting of three N atoms from a planar pzcq and three C atoms from three CN groups. The bond lengths of Fe–C(cyanide) are in the ranges of  $1.964\text{--}1.970\text{ \AA}$  for **1** and

$1.938\text{--}1.959\text{ \AA}$  for **2**, which demonstrate that the coordination of the blocked building unit to the metal ions gives rise to the enhanced C–N bond order as checked by the IR spectra. The obtained bond distances are consistent with those of the related  $[\text{Fe}(\text{bpca})(\text{CN})_3]^-$  and  $[\text{Fe}(\text{pcq})(\text{CN})_3]^-$  compounds.<sup>10,11</sup> The Fe–N(amide) distance ( $1.88\text{--}1.89\text{ \AA}$ ) is significantly shorter than the other two Fe–N lengths ( $1.94\text{--}1.96\text{ \AA}$ ) associated with pzcq, which is due to the presence of a strong  $\sigma$ -donor effect of the deprotonated amide. The Fe–CN bond angles are almost linear ( $172.4\text{--}178.1^\circ$ ). The  $[\text{Fe}(\text{pzcq})(\text{CN})_3]^-$  moiety can behave as a bridging group between  $[\text{Mn}(\text{salen})]^+$  entities in the cis mode, and the resultant self-assembly process leads to a neutral one-dimensional chain with a zigzag structural pattern. In the  $[\text{Mn}(\text{salen})]^+$  unit, the Mn atom can be viewed as a distorted octahedral geometry based on equatorial  $\text{N}_2\text{O}_2$  donor atoms from salen [ $\text{Mn1}\text{--O2} = 1.885(3)\text{ \AA}$ ,  $\text{Mn1}\text{--O3} = 1.878(3)\text{ \AA}$ ,  $\text{Mn1}\text{--N9} = 1.985(3)\text{ \AA}$ , and  $\text{Mn1}\text{--N10} = 1.983(3)\text{ \AA}$ ] and two apical N atoms from bridging CN groups [ $\text{Mn1}\text{--N1} = 2.288(3)\text{ \AA}$  and  $\text{Mn1a}\text{--N3} = 2.263(3)\text{ \AA}$ ; a,  $-x + 0.5, y - 0.5, -z + 0.5$ ]. The axial elongation accounts for the existence of the well-known Jahn–Teller effect on an octahedral high-spin  $\text{Mn}^{\text{III}}$  ion.<sup>16</sup> The bridging CN groups form two Mn–NC angles of  $152.2(3)^\circ$  for  $\text{Mn1}\text{--N1}\text{--C1}$  and  $158.3(3)^\circ$  for  $\text{Mn1a}\text{--N3}\text{--C3}$  within a chain. These results are compared with the cyanide-linked  $\text{Fe}^{\text{III}}\text{--Mn}^{\text{III}}$  chain containing the facial  $[\text{Fe}(\text{Tp})(\text{CN})_3]^-$  anion in which two Mn–NC angles are more different by  $10^\circ$ .<sup>17</sup> The torsion angles are  $-2(4)^\circ$  for  $\text{Fe1}\text{--C1}\text{--N1}\text{--Mn1}$  and  $75(3)^\circ$  for  $\text{Fe1}\text{--C3}\text{--N3}\text{--Mn1a}$ . The distances between Fe and Mn ions on the same chain, separated through the CN links, are similar,  $5.179(1)\text{ \AA}$  for  $\text{Fe1}\text{--Mn1}$  and  $5.240(1)\text{ \AA}$  for  $\text{Fe1}\text{--Mn1a}$ . The angle between the elongated axes of the neighboring  $\text{Mn}^{\text{III}}$  ions within the chain is  $110.6^\circ$ . The shortest interchain Fe–Fe separation between nearby chains is  $7.194\text{ \AA}$ . The  $\pi\text{--}\pi$  contacts between the two C atoms (C4 and C5) on the pyridyl groups of pzcq ligands in disparate adjacent chains, which run parallel with the chains in most proximity, are not substantial. This is because the Fe–Fe distance of  $8.001\text{ \AA}$  via the  $\pi\text{--}\pi$  interactions is even larger than the shortest interchain Fe–Fe spacing (Figure S2 in the Supporting Information).

The effective magnetic moment of **1** at  $1000\text{ G}$  is  $2.12\text{ } \mu_{\text{B}}$ , which is larger than the spin-only value ( $1.73\text{ } \mu_{\text{B}}$ ) for a low-spin  $\text{Fe}^{\text{III}}$  (Figure S3 in the Supporting Information). As the temperature decreases, the moment gradually declines, indicating characteristic unquenched orbital angular momentum of octahedral low-spin  $\text{Fe}^{\text{III}}$  systems.<sup>4,8</sup>

As illustrated in Figure 2, thermal variation of the magnetic susceptibility for **2** was collected in the temperature range of  $2\text{--}300\text{ K}$  at  $1\text{ kG}$ . The  $\chi_{\text{m}}T$  value of  $3.347\text{ cm}^3\text{ K mol}^{-1}$  is somewhat smaller than the theoretical one ( $3.375\text{ cm}^3\text{ K mol}^{-1}$ ) calculated from one isolated  $\text{Fe}^{\text{III}}$  ( $S_{\text{Fe}} = 1/2$ ) spin and

(14) Lim, J. H.; Kang, J. S.; Kim, H. C.; Koh, E. K.; Hong, C. S. *Inorg. Chem.* **2006**, *45*, 7821.

(15) Crystal data for **1**:  $\text{C}_{41}\text{H}_{29}\text{FeN}_7\text{O}_7$ ,  $M_r = 722.53$ , monoclinic, space group  $P2_1/c$ ,  $a = 8.6018(2)\text{ \AA}$ ,  $b = 15.0530(4)\text{ \AA}$ ,  $c = 27.7637(6)\text{ \AA}$ ,  $\beta = 108.0480(10)^\circ$ ,  $V = 3418.04(14)\text{ \AA}^3$ ,  $Z = 4$ ,  $\rho_{\text{calcd}} = 1.404\text{ g cm}^{-3}$ ,  $\mu = 0.534\text{ mm}^{-1}$ ,  $T = 130\text{ K}$ , 17 400 reflections collected, 8041 unique ( $R_{\text{int}} = 0.02796$ ),  $R1 = 0.0417$ ,  $wR2 = 0.1082$  [ $I > 2\sigma(I)$ ]. Crystal data for **2**:  $\text{C}_{33}\text{H}_{29}\text{FeMnN}_9\text{O}_7$ ,  $M_r = 774.44$ , monoclinic, space group  $P2_1/n$ ,  $a = 14.5107(3)\text{ \AA}$ ,  $b = 12.1967(3)\text{ \AA}$ ,  $c = 19.3412(5)\text{ \AA}$ ,  $\beta = 91.4450(10)^\circ$ ,  $V = 3421.97(14)\text{ \AA}^3$ ,  $Z = 4$ ,  $\rho_{\text{calcd}} = 1.503\text{ g cm}^{-3}$ ,  $\mu = 0.855\text{ mm}^{-1}$ ,  $T = 130\text{ K}$ , 34 193 reflections collected, 8500 unique ( $R_{\text{int}} = 0.0709$ ),  $R1 = 0.0622$ ,  $wR2 = 0.1451$  [ $I > 2\sigma(I)$ ].

(16) (a) Yoon, J. H.; Lim, J. H.; Kim, H. C.; Hong, C. S. *Inorg. Chem.* **2006**, *45*, 9613. (b) Ko, H. H.; Lim, J. H.; Kim, H. C.; Hong, C. S. *Inorg. Chem.* **2006**, *45*, 8847.

(17) Wang, S.; Ferbinteanu, M.; Yamashita, M. *Inorg. Chem.* **2007**, *46*, 610.

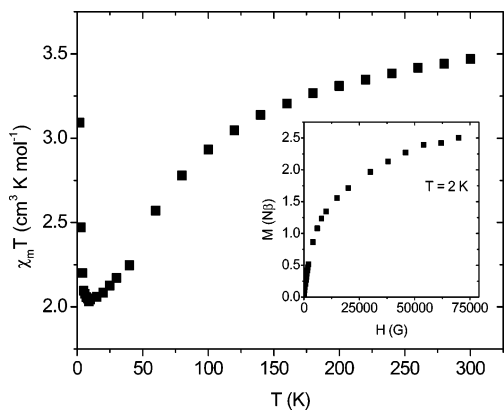


**Figure 2.** Plot of  $\chi_m T$  versus  $T$  of **2**. The inset shows the field dependence of the magnetization at 2 K.

one  $\text{Mn}^{\text{III}}$  ( $S_{\text{Mn}} = 2$ ) spin with  $g = 2$ . Lowering the temperature causes  $\chi_m T$  to be diminished down to  $2.032 \text{ cm}^3 \text{ K mol}^{-1}$  at 9 K, clearly suggesting the existence of intrachain antiferromagnetic interactions between Fe and Mn centers transmitted by CN bridges. It is worth noting that the magnetic behavior at  $T > 9 \text{ K}$  is in contrast to ferromagnetic interactions observed in the  $\text{Fe}^{\text{III}}\text{--Mn}^{\text{III}}$  chain formed by a *fac*- $[\text{Fe}(\text{Tp})(\text{CN})_3]^-$  anion and most of the other related  $\text{Fe}^{\text{III}}\text{--Mn}^{\text{III}}$  systems.<sup>17,18</sup> It appears that the  $\text{Fe}^{\text{III}}\text{--C}\equiv\text{N--Mn}^{\text{III}}$  unit can provide either antiferromagnetic or ferromagnetic alignments depending on the subtle structural variations present in bridging pathways.<sup>18</sup> An abrupt rise in  $\chi_m T$  below the minimum temperature is obviously relevant with the pronounced correlation of noncompensated spins along the chain, which is normally observed in ferrimagnetic systems.<sup>19</sup> The Curie–Weiss law can be applicable to the linear part of the inverse magnetic susceptibility data (40–300 K). It affords  $C = 3.794 \text{ cm}^3 \text{ K mol}^{-1}$  and  $\theta = -28.9 \text{ K}$ , signifying the existence of antiferromagnetic couplings between neighboring magnetic centers (Figure S4 in the Supporting Information).<sup>20</sup> To get further insight into the underlying magnetic nature in **2**, the field dependence of the magnetization at 0–7 T and 2 K was investigated (inset of Figure 2). The magnetization data per FeMn display a constant increase as the field is raised, reaching a value of  $2.51 N\beta$  at 7 T, which is slightly smaller than the theoretical value of  $3 N\beta$  obtained from the ferrimagnetic consequence ( $gS_{\text{Mn}} - gS_{\text{Fe}}$ ), assuming  $g = 2$ . The reduced magnetization versus  $H/T$  plots show that the isofield curves are not superimposed (Figure S5 in the Supporting Information).

- (18) (a) Miyasaka, H.; Ieda, H.; Matsumoto, N.; Re, N.; Crescenzi, R.; Floriani, C. *Inorg. Chem.* **1998**, *37*, 255. (b) Miyasaka, H.; Matsumoto, N.; Re, N.; Gallo, E.; Floriani, C. *Inorg. Chem.* **1997**, *36*, 670. (c) Ni, W.-W.; Ni, Z.-H.; Cui, A.-L.; Liang, X.; Kou, H.-Z. *Inorg. Chem.* **2007**, *46*, 22. (d) Ni, Z.-H.; Kou, H.-Z.; Zhang, L.-F.; Ge, C.; Cui, A.-L.; Wang, R.-J.; Li, Y.; Sato, O. *Angew. Chem., Int. Ed.* **2005**, *44*, 7742.
- (19) (a) Yoon, J. H.; Kim, H. C.; Hong, C. S. *Inorg. Chem.* **2005**, *44*, 7714. (b) Zhang, Y.-Z.; Gao, S.; Wang, Z.-M.; Su, G.; Sun, H.-L.; Pan, F. *Inorg. Chem.* **2005**, *44*, 4534. (c) Zhang, Y.-Z.; Gao, S.; Sun, H.-L.; Su, G.; Wang, Z.-M.; Zhang, S.-W. *Chem. Commun.* **2004**, 1906.
- (20) Given that  $\text{Mn}^{\text{III}}$  and  $\text{Fe}^{\text{III}}$  spins are antiparallel,  $\text{Mn}^{\text{III}}$  was assumed to act as a classical spin carrier with  $S_{\text{Mn}} = 2$ , leading to an effective alternating chain with  $S_{\text{Mn}} = 2$  and  $S_{\text{Fe}} = 1/2$ . This approximation gave poor parameters of  $g_{\text{Mn}} = 1.99$ ,  $g_{\text{Fe}} = 2.99$ , and  $J = -17.2 \text{ cm}^{-1}$ ,<sup>13</sup> so that the magnetic model may be roughly applied to the system with the quantum spin  $S_{\text{Fe}} = 1/2$ .

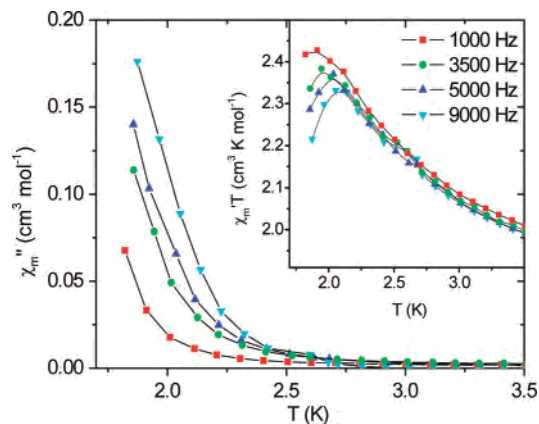


**Figure 3.** Plot of  $\chi_m''$  versus  $T$  of **2** at an ac field of 5 G, zero dc field, and several indicated frequencies. The inset represents the temperature dependence of  $\chi_m' T$ .

To examine the spin dynamics for **2**, alternating current (ac) susceptibility was recorded at zero dc field and an ac field of 5 G with oscillating frequencies. As depicted in Figure 3, the frequency-dependent out-of-phase term ( $\chi_m''$ ) in the ac data was discernible below 2.7 K. Increasing the frequency from 1000 to 9000 Hz renders the magnitude of  $\chi_m''$  to grow gradually with no maxima visible even at 1.8 K.<sup>21</sup> The advent of the nonzero  $\chi_m''$  component is concerned with spin glasses, long-range ferromagnetic orderings, and single-chain magnets. The fact that **2** is crystalline without structural disorder precludes the possibility of a spin glass. The shift of the peak temperature ( $=T_{\text{max}}$ ) in  $\chi_m' T$  and the estimated quantity may favor single-chain magnet characters rather than long-range ferromagnetic order, but it remains elusive at this stage.<sup>21</sup>

In summary, we have successfully prepared a new molecular building block,  $[\text{Fe}(\text{pzcq})(\text{CN})_3]^-$  (**1**), and a one-dimensional bimetallic compound,  $[\text{Fe}(\text{pzcq})(\text{CN})_3][\text{Mn}(\text{salen})]\cdot 4\text{H}_2\text{O}$  (**2**), with a zigzag chain structure. Noticeably, intrachain antiferromagnetic couplings through the  $\text{Fe}^{\text{III}}\text{--CN--Mn}^{\text{III}}$  pathways are operative in **2**. The molecular precursor, *mer*- $[\text{Fe}(\text{pzcq})(\text{CN})_3]^-$ , may be one of the good building units to produce single-chain magnets when non-covalent contacts between chains are completely suppressed.

**Acknowledgment.** This work was supported by the Korea Science and Engineering Foundation (KOSEF) grant funded by the Korea government (MOST; Grant R01-2007-000-10240-0). C.S.H. thanks Dr. Wolfgang Wernsdorfer for the valuable comments in measuring low-temperature magnetic properties.

**Supporting Information Available:** X-ray crystallographic file in CIF format and additional synthetic, structural, and magnetic data for **1** and **2**. This material is available free of charge via the Internet at <http://pubs.acs.org>.

IC701361A

- (21) If we applied the equation  $\phi = \Delta T_{\text{max}}/T_{\text{max}}\Delta(\log f)$  to the  $\chi_m' T$  product in **2**,  $\phi$  was estimated as 0.11, which is close to a superparamagnet. However, as judged by the current ac data of **2**, one might see a tiny hysteresis at low temperature ( $T < 1.8 \text{ K}$ ), but it is not very clear whether this is due to the SCM nature or interchain coupling (dipolar and/or exchange coupling).